Eur. Phys. J. B **12**, 405–411 (1999)

**THE EUROPEAN PHYSICAL JOURNAL B**

EDP Sciences


# Encapsulation of filaments of a self-assembling bicopper complex in polymer nanowires

D. Lopez[a] and J.-M. Guenet[b]

Laboratoire de Dynamique des Fluides Complexes, Université Louis Pasteur[c], 4 rue Blaise Pascal, 67070 Strasbourg Cedex, France

Received 20 January 1999 and Received in final form 14 May 1999

**Abstract.** We report on the preparation conditions and the characterization by calorimetry and small-angle neutron scattering of a molecular composite material obtained via the heterogeneous nucleation of the fibrils of a thermoreversible gel. This physical process allows encapsulation of monomolecular filaments of a self-assembling bicopper complex into nanosized polymer fibrils. Due to the existence of 1-D arrangements of copper atoms, this material may possess unusual magnetic properties (spin ladders).

**PACS.** 81.05.-t Specific materials: fabrication, treatment, testing and analysis – 82.70.Gg Gels and sols – 61.41.+e Polymers, elastomers, and plastics

## Introduction

The making of nanosized materials with specific properties is currently a challenging issue. New morphologies and molecular structures are produced either by using physical effects, such as polymer-solvent compound formation for producing highly-adsorbing polymer chlathrates [1], or through chemical reaction as is the case for fullerenes nanotubes [2]. Here, we report on a method relying upon the phenomenon of heterogeneous nucleation which allows preparation of a composite fibrillar material, where a bicopper complex monomolecular filament is encapsulated within a polymer sheath. The bicopper complex filament acts as the heterogeneous nucleus for nucleating the growth of the fibrillar structure of a thermoreversible gel.

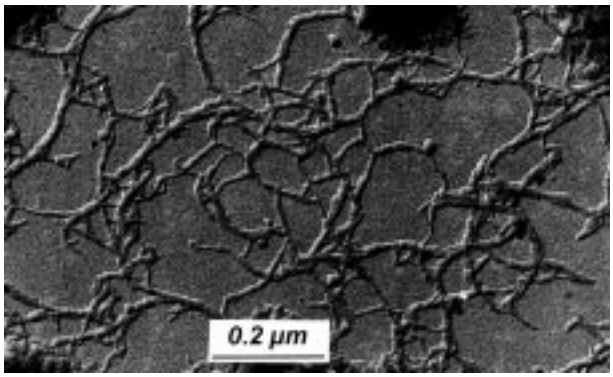


**Fig. 1.** Electron micrograph of an iPS xerogel. Scale as indicated.

*Isotactic polystyrene*, a highly-stereoregular polymer, can produce thermoreversible gels of fibrillar morphology [3,4] in appropriate organic solvents such as trans-decalin (see Fig. 1). The mesh size is typically in the range $0.1-1\,\mu$m, while the fibrils possess cross-section radii in the nanosize domain (2 to 20 nm). Within the fibrils the chains take on a worm-like conformation with a persistence length of about $l_\mathrm{p} \approx 4$ nm, *i.e.* 4 times larger than the value in the unperturbed state [5]. Gelation sets in rather than the formation of chain-folded crystals because the chains already possess a worm-like conformation in the *sol* state. This eventually impedes them from folding on cooling, hence the formation of fibrils instead of spherulites. Several results suggest that the occurrence of such a large persistence length in the sol state arises from the existence of a solvation shell around the chains that stabilize the $3_1$ helical form [6–8].

The *bicopper complex* portrayed in Figure 2 generates monomolecular thread-like structures in a large variety of organic solvents, among which *trans*-decalin [9]. Due to the low interaction energy between consecutive bicopper complex molecules (about $kT$), any given filament has a limited lifetime defined by a breaking time $\tau_\mathrm{b}$ of about 1 s. Although the rheological properties of these solutions are very similar to those observed for classical polymers, stress relaxation occurs through two mechanisms: *reptation* and *breaking/reformation* [10]. New filaments are

[a] *Permanent address*: Instituto de Ciencia y Tecnologia de Polimeros, CSIC, Juan de la Cierva 4, 28006 Madrid, Spain

[b] *Present address*: Institut de Chimie des Surfaces et Interfaces, CNRS UPR 9069, BP 2488, 15 rue Jean Starcky, 68057 Mulhouse Cedex, France
e-mail: `jm.guenet@univ-mulhouse.fr`

[c] CNRS UMR 7506

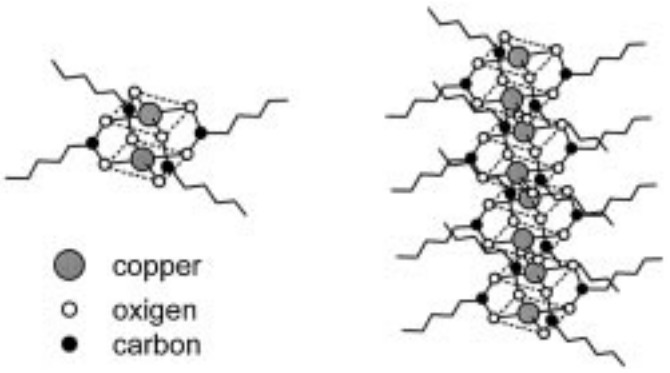


**Fig. 2.** The bicopper complex molecular structure and the columnar structure resulting from their piling process [18].

ceaselessly produced from the remnants of older ones so that these systems are accordingly designated as "living" polymers [10].

The encapsulation of the bicopper complex filaments in a polymer sheath has two decisive advantages: i) the lifetime of the filaments is to become infinite, and ii) the gel matrix is an appropriate medium for fibre spinning [11], which should pave the way for further large-scale developments.

## Experimental

### Materials

The hydrogenous (iPSH) and deuterated (iPSD) isotactic polystyrene samples used in this study were synthesized by means of Natta's method [12]. The weight-average molecular weights as determined by SEC in THF at 25 °C were found to be: $M_w = 427\,000$ g/mol with $M_w/M_n = 2.55$ for iPSH and $M_w = 166\,000$ g/mol with $M_w/M_n = 2.92$ for iPSD.

The bicopper complex (copper (II) 2-ethylhexanoate) was synthesized and purified by a method devised by Martin and Waterman [13]. Hydrogenous *trans*-decalin was purchased from Aldrich while deuterated *trans*-decalin was obtained from Eurisotop (Saclay, France). They were used without further purification.

### Sample preparation and techniques

#### Differential scanning calorimetry (DSC)

Homogeneous solutions were prepared by heating appropriate mixtures of *iPSH+bicopper complex+hydrogenated solvent* in hermetically closed test-tubes at 150 °C. Gels were formed by subsequent quench of these solutions at room temperature. Pieces of gel were then transfered into aluminium DSC pans that were hermetically sealed. Thermal analysis was carried out with a DSC 30 from METTLER equipped with the TA9000 pilot system and a TA72 software for processing the raw data. Prior to any measurement gels were melted in the DSC pan in order to erase all structures. Samples were then scanned from 150 to −70 °C at different cooling or heating rates: 15, 10, 5 and 2.5 K/min.

*Small-angle neutron scattering.* The experiments were performed on the PAXE camera located at the Laboratoire Léon Brillouin (LLB) (CEN Saclay, France). A wavelength of $\lambda_m = 0.6$ nm was used with a wavelength distribution characterized by a full width at half maximum, $\Delta\lambda/\lambda_m$, of about 10%. Neutron detection and counting was achieved with a built-in two-dimensional sensitive detector composed of $64 \times 64$ cells (further details are available on request at LLB). By varying the sample-detector distance the available $q$-range was $0.1 < q\ (\mathrm{nm}^{-1}) < 2.5$ where $q = (4\pi/\lambda)\sin(\theta/2)$, $\theta$ being the scattering angle.

Gels samples were prepared directly in sealable quartz cells from HELLMA of optical paths of 1 and 2 mm. After introducing appropriate mixtures of the different constituents, the system was heated up to 150 °C to obtain homogeneous solutions. Gelation was achieved by a quench to 0 °C.

By toying with the scattering amplitude of the solvent, the nanostructure of either the polymer gel or the bicopper complex can be determined. 1) *Polymer gel structure*: a match of the coherent scattering amplitude of the hydrogenous bicopper complex was achieved by using a solvent isotopic mixture of deuterated (tdecaD) and hydrogenous *trans*-decalin (tdecaH) (tdecaD/tdecaH = 8/92 in v/v) leaving only the coherent intensity arising from the deuterated polymer gel. 2) *Bicopper complex structure*: A highly-deuterated solvent mixture (91% tdecaD/9% tdecaH in v/v) was used for matching the coherent scattering amplitude of the deuterated polymer gel, thus leaving only the coherent scattering of the bicopper complex.

The position sensitive detector was calibrated by means of hydrogenous *cis*-decalin which gives off only incoherent scattering. Under these conditions the absolute intensity, $I_A(q)$ is written:

$$I_A(q) = I_N(q)/K \tag{1}$$

in which $I_N(q)$ is the intensity obtained after background subtraction, transmission corrections and detector normalization, and $K$ is a constant which reads:

$$K = \frac{4\pi(a_i - y a_s)^2 \delta_{dec} T_{dec} N_A}{g(\lambda_m)(1 - T_{dec}) m_i^2} \tag{2}$$

in which $a_i$ is the coherent scattering amplitude of either the polymer or the bicopper complex, and $a_s$ the scattering coherent amplitude of the solvent mixture, $\delta_{dec}$ and $T_{dec}$ the thickness and the transmission of the calibration *cis*-decalin sample, $m_i$ the molecular weight of the scattering unit (polymer or bicopper complex), and $g(\lambda_m)$ a constant which is camera-dependent and was measured by using Cotton's method [14]. Here, $I_A(q)$ is dimensionless because of the expression of $K$ for which the incoherent scattering of the calibration sample is included.

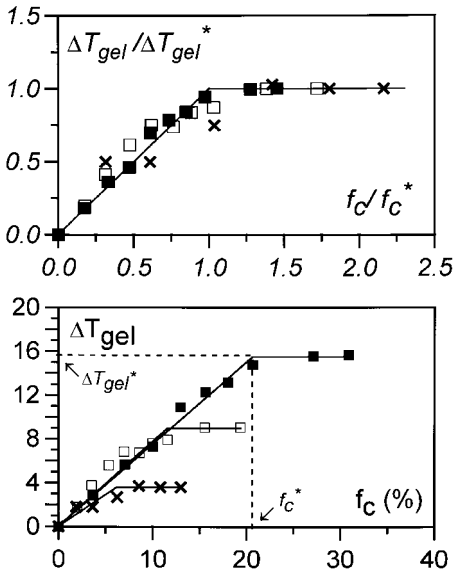


**Fig. 3.** *Lower*: increase of the gelation temperature as a function of the bicopper complex mole fraction (with respect to the mixture polymer+complex) for different polymer concentrations ((■) 0.04 g/cm$^3$; (□) 0.08 g/cm$^3$; (×) 0.16 g/cm$^3$). For $C_{\rm pol} = 0.04$ g/cm$^3$, $C_{\rm Cu}$ varies from 0.01 g/cm$^3$ to 0.12 g/cm$^3$. $f_{\rm c}^*$ corresponds to the cross-over. *Upper*: an universal curve is obtained by plotting $\Delta T_{\rm gel}/\Delta T_{\rm gel}^*$ *vs.* $f_{\rm c}/f_{\rm c}^*$, where $\Delta T_{\rm gel}^*$ corresponds to the leveling-off temperature.

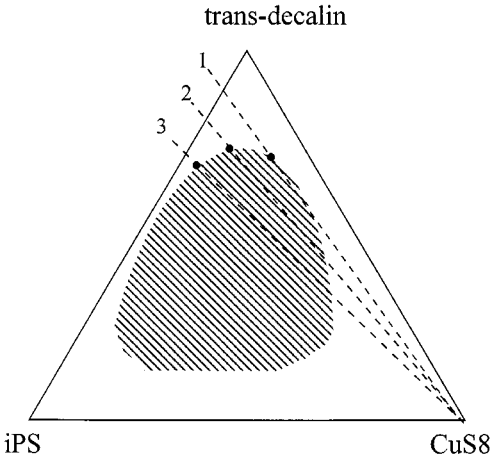


**Fig. 4.** Hypothetical ternary phase diagram at constant temperature. The cross-hatched area stands for the miscibility gap. The dotted lines represent the locus where the ratio polymer/solvent is a constant while the fraction of bicopper complex can be altered. Demixing should therefore occur at lower bicopper fractions (as indicated by dots) on increasing the polymer concentration.

## Results and discussion

### Thermodynamic study

The gelation threshold of isotactic polystyrene solutions in *trans*-decalin stands close to 20 °C. DSC thermogrammes display a formation exotherm whose maximum is cooling-rate dependent [3]. The "equilibrium" gelation threshold, $T_{\rm gel}$, is determined by extrapolation at zero cooling rate. The use of quotation marks is required because, strictly speaking, an infinitely-slow cooling rate would not give a gel structure but a spherulitic texture instead (see Ref. [3] for further details). Here extrapolation to zero-heating rate allows one to overcome heat transfer effects that can differ from one sample to another. (Note that the gelation temperature is not molecular weight dependent within experimental uncertainties [3].) As the melting of these gels occurs some 30 °C above the gelation threshold, gelation might be a homogeneously-nucleated process. Addition of molecules that would act as heterogeneous nuclei should therefore increase the gelation temperature.

In the case of the ternary system iPS/Cu2S8/*trans*-decalin the "equilibrium" gelation threshold can thereby be determined as a function of the fraction $f_{\rm c}$ of bicopper complex ($f_{\rm c} = n_{\rm CuS8}/(n_{\rm CuS8} + n_{\rm iPS})$, with $n_{\rm CuS8}$ = number of moles of bicopper complex and $n_{\rm iPS}$ = number of moles of iPS). The parameter of interest is the difference $\Delta T_{\rm gel}$ between the gelation threshold of the ternary system with respect to the binary mixture's (*i.e.* the solvent+polymer). The addition of bicopper complex increases the gelation threshold as shown in Figure 3. $\delta T_{\rm gel}$ varies nearly linearly up to some *critical bicopper molar fraction* $f_{\rm c}^*$, and then levels off. The increase of the gelation threshold by addition of a potential nucleating agent reveals the occurrence of a heterogenous nucleation process (for further reading see Refs. [15,16]). That the bicopper complex nucleates the gelation of polystyrene is borne out by two additional results: the gel melting enthalpy and the gel melting temperature are independent of the bicopper content.

The existence of a two-regime behaviour as shown in Figure 3 is seen to be independent of the polymer concentration, yet the critical fraction $f_{\rm c}^*$ is: the higher the polymer concentration, the lower the critical bicopper fraction (see Fig. 3). The leveling-off arises from the fact that the bicopper filaments and the polymer are no longer compatible above a given bicopper fraction as observed with atactic polystyrene (this variety of polystyrene does not form gels in *trans*-decalin). Consequently, further addition of bicopper complex is rejected into another microphase (polymer-poor phase), and becomes useless for nucleation purposes, hence the levelling-off of $\Delta T_{\rm gel}$. The incompatibility increases with increasing polymer concentration. A hypothetical ternary phase diagram drawn in Figure 4 illustrates this point. The occurrence of a phase separation will be further borne out by the scattering experiments obtained on the structure of the bicopper complex for $f = 2f_{\rm c}^*$.

At high temperature homogeneous, transparent solutions are obtained which indicates that bicopper complex molecules display a high degree of compatibility with isotactic polystyrene. On decreasing temperature bicopper complex molecules start to pile up well-above the polymer gelation threshold and produce rod-like filaments within a solution of polymer chains that are already locally rigid. The increase of the gelation temperature suggests that these filaments act as nuclei for the aggregation of polymer

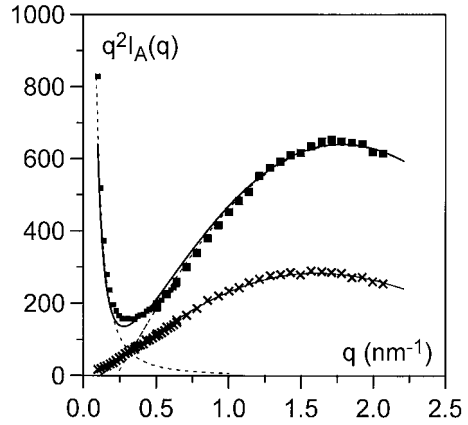


**Fig. 5.** Neutron scattering curves obtained for the *bicopper complex* plotted by means of a Kratky representation ($q^2I(q)$ *vs.* $q$). (×) for $f_c = f_c^*$ and (■) for $f_c = 2f_c^*$. The solid line for corresponds to the best fit with equation (3). The dotted lines are calculated with equations (6, 7) for $f_c = 2f_c^*$ (see text for details). The solid line for $f_c = 2f_c^*$ corresponds to the sum of these two contributions.

chains and are encapsulated in a polymer sheath. Heterogeneous nucleation has another consequence: the size (*i.e.* the cross-section) of these fibrils should decrease because of the increase of the nucleation sites (see Refs. [15,16] for details). These effects can be directly tested by performing scattering experiments.

It is worth mentioning that heterogenous nucleation of polymer crystallization by long-rod-like filaments through a similar mechanism has already been reported for chain-folded-crystals in bulk polyethylene [17], but, to the best of our knowledge, this is the first report of a similar effect for thermoreversible gelation.

## Molecular organization. Nanostructure

### Bicopper complex in the gel matrix

As has been already established by Dammer *et al.* [18], the bicopper complex forms long, rod-like monomolecular filaments in *trans*-decalin with a mean-length $\langle L\rangle \approx 9$ nm. The nearly-maxwellian rheological behaviour observed by Terech *et al.* [9] and Dammer *et al.* [18] hints, however, at the existence of a fraction of filaments much longer than $\langle L\rangle$ in the solution.

Scattering curves obtained on samples prepared at $f_c = f_c^*$ and at $f_c = 2f_c^*$ are shown in Figure 5 (here only the coherent scattering of the bicopper complex is detectable). As can be seen the scattered intensity in the high-$q$ range is similar while a significant upturn is seen in the low-$q$ domain for $f_c = 2f_c^*$.

The scattering curve for $f_c = f_c^*$ can be fitted by considering a solid-cylinder model of cross-section radius $r_H$. For $qL > 1$ and $L > r_c$, the theoretical scattering intensity is written [19]:

$$q^2I(q) \propto C_{Cu}\mu_L \frac{4J_1^2(qr_c)}{q^2r_c^2}\left[\pi q - \frac{2}{\langle L\rangle}\right] \qquad (3)$$

in which $\mu_L$ is the mass per unit length and $C_{cu}$ the bicopper complex concentration. The mean length $\langle L\rangle$ is simply given through:

$$\langle L\rangle = \frac{2}{\pi q_0} \qquad (4)$$

in which $q_0$ is the intercept for $q^2I(q) = 0$ with the $q$-axis of the linear section (for $qr_c < 1$).

Typical values of $r_H$ and $\mu_L$ are $r_c = 0.82 \pm 0.02$ and $\mu_L = 1290$ to 1520 g/mol nm that definitely point to the occurrence of a monomolecular filament nanostructure [9]. As expected from the heterogenous nucleation process, *monomolecular filaments of bicopper complex are therefore trapped within a polymer sheath.* They now possess an infinite lifetime as opposed to their former status in solution [18]. Their mean-length is $\langle L\rangle \approx 6$ nm, that is shorter by about 30% than that occurring in the non-encapsulated state. Note that the value of $\langle L\rangle$ is very close to that of the chains persistence length, an effect which might not be totally fortuitous but related to the nucleation process.

The scattering curve for $f_c = 2f_c^*$ can be accounted for by considering a two-population system: monomolecular filaments and three-dimensional objects. The theoretical intensity is then written:

$$q^2I(q) \propto X\frac{S}{Vq^2} + (1-X)C_H\mu_L\frac{4J_1^2(qr_c)}{q^2r_c^2}\left[\pi q - \frac{2}{\langle L\rangle}\right] \qquad (5)$$

in which $X$ is the fraction of those three-dimensional objects, $S/V$ their ratio *surface/volume*. All the other symbols are defined in equation (3). Such an equation gives off an upturn at small angles while the second term predominates at larger angles. Typically two regimes are expected and actually seen (see dotted lines Fig. 5):

$$\text{for } q\langle L\rangle < 1 \qquad q^2I(q) \propto X\frac{S}{Vq^2} \qquad (6)$$

$$\text{for } q\langle L\rangle > 1$$

$$q^2I(q) \propto (1-X)C_H\mu_L\frac{4J_1^2(qr_c)}{q^2r_c^2}\left[\pi q - \frac{2}{\langle L\rangle}\right]\cdot \qquad (7)$$

Note that no cross term is needed in equation (5) for fitting the experimental data. This implies that demixing occurs on a much larger distance scale than that explored in the SANS experiments. That two different states for the bicopper complex coexist implies the existence of two phases, a conclusion already reached from the thermodynamic study. Clearly, above the critical bicopper complex fraction $f_c > f_c^*$ only a part of the complex efficiently acts as a nucleating agent while the excess is rejected into another phase and most probably forms three-dimensional crystals as those described by Abied *et al.* [20]. Of further note is the shortening of the mean length of the filaments (here $\langle L\rangle \approx 3$ nm)

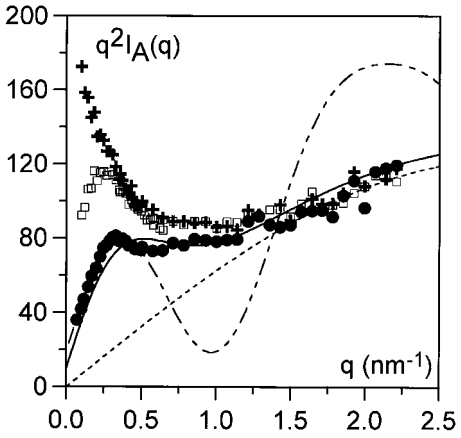


**Fig. 6.** Neutron scattering curves obtained for the *polymer* plotted by means of a Kratky representation ($q^2I(q)$ *vs.* $q$). (+) for $f_c = 0$, (□) for $f_c = f_c^*$ and (⧫) for $f_c = 2f_c^*$. The dashed lines represent the expected intensity for the model portrayed in Figure 6 by using the two asymptotic regimes ((- - - -) for $ql_0 > 1$ and (– - - –) for $q\sigma < 1$). The solid line is obtained by using equation (12) which introduces frozen fluctuations of the interchains distance around the most probable distance $l_0$ (see text for details).

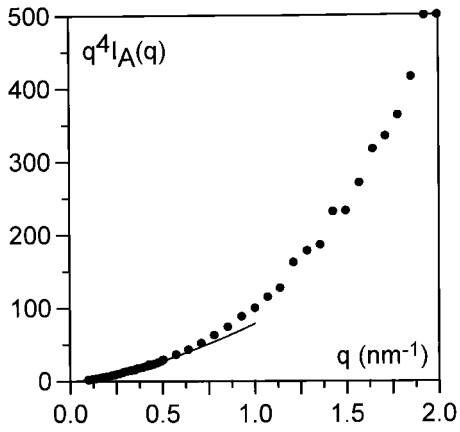


**Fig. 7.** Neutron scattering curves obtained for the polymer in the absence of bicopper complex plotted by means of a $q^4I(q)$ *vs.* $q$ representation. The curve is fitted by means of relation (5) in the transitional range (namely for $q < 0.5$ nm$^{-1}$).

## Polymer nanostructure

Typical scattering curves obtained on gels are displayed in Figure 6 by means of a $q^2I(q)$ *vs.* $q$ representation (this time only the polymer coherent signal is detectable). The scattering curve of the non-nucleated gel (*i.e.* in the absence of bicopper complex) reveals two regimes: at low angle an upturn which is consistent with the fibrillar structure of these gels, and at large angle a rod- like behaviour which indicates that chains in these fibrils possess large persistence length and are separated by a solvation sheath (see Ref. [5] for further details). A typical distance between neighbouring chains is about 2 nm [21].

The low-angle domain can be fitted by using equation (8) recently derived by Guenet [22] for systems of fibrils displaying cross-section polydispersity of the type $w(r) \sim r^{-\lambda}$ (with $0 < \lambda < 3$) bounded by two cut-off radii $r_{\max}$ and $r_{\min}$. This approach can be applied here as in the $q$-range explored the intensity is only sensitive to fibrils' cross-sections. The intensity is then written for $qL > 1$ and $qr_{\max} > 1$ (designated as transitional regime):

$$\frac{q^4 I_{\mathrm{A}}(q)}{C_{\mathrm{p}}} = 4\pi^2\rho\left[A(\lambda)q^{\lambda} - \frac{1}{\lambda r_{\max}^{\lambda}}\right] \Big/ \int_{r_{\min}}^{r_{\max}} w(r)\mathrm{d}r \quad (8)$$

where $C_{\mathrm{p}}$ is the polymer concentration and $\rho$ is the molecular density of the fibrils. $A(\lambda)$ reads:

$$A(\lambda) = \frac{\Gamma(\lambda)\Gamma\left(\dfrac{3-\lambda}{2}\right)}{2^{\lambda}\Gamma\left(\dfrac{\lambda+1}{2}\right)\Gamma\left(\dfrac{\lambda+3}{2}\right)\Gamma\left(\dfrac{\lambda+1}{2}\right)}\cdot \quad (9)$$

The fit can be achieved by taking $\lambda = 3/2$, from which is derived the following expression for $r_{\max}$ (see Fig. 7):

$$r_{\max} = \frac{0.642}{q_0} \quad (10)$$

where $q_0$ is the intercept with the $q$-axis in a $q^4I(q)$ *vs.* $q$ representation. Typical values for $r_{\max}$ are located somewhere between 10 and 15 nm in agreement with electron microscopy findings (the uncertainty on the determination of $q_0$ does not allow one to measure $r_{\max}$ with a better accuracy). Value of $r_{\min}$ cannot be measured due to the absence of a Porod-regime.

In the large angle domain, the rod-like regime takes over and the scattering curve can be fitted with equation (3) which is also valid for helices in the investigated $q$-range (low resolution [19]). This yields a mass per unit length $\mu_{\mathrm{L}} = 520 \pm 50\,\mathrm{g\,mol^{-1}nm^{-1}}$ corresponding to chains under *a near*-$3_1$ helical conformation as already found in previous studies [3,21].

Addition of bicopper complex causes a significant decrease of the upturn at low angle which implies a decrease in size, the most likely effect being a decrease of fibrils cross-section (see Fig. 6). The scattering curve is now seen in the low-$q$ domain to vary as:

$$q^2I(q) = C_{\mathrm{p}}\mu[qf(q\sigma) + z(q)] \approx C_{\mathrm{p}}\mu[qf(q\sigma) + \text{const.}] \quad (11)$$

where $\mu$ is a mass per unit length, $f(q\sigma) \approx 1$, $\sigma$ is some kind of cross-section, and $z(q) \approx$ const. in the explored $q$-range. This type of variation can be further confirmed by means of a Porod-plot Log $qI(q)$ *vs.* $q^2$ shown in Figure 8. The existence of a linear variation at low $q$ is consistent with a cross-sectional effect and allows determination of the value of $\sigma$.

Note that if the increase of the gel threshold $T_{\mathrm{gel}}$ were merely due to a phase separation phenomenon between the polymer and the bicopper complex, then one would observe an increase of the fibrils cross-sections instead.

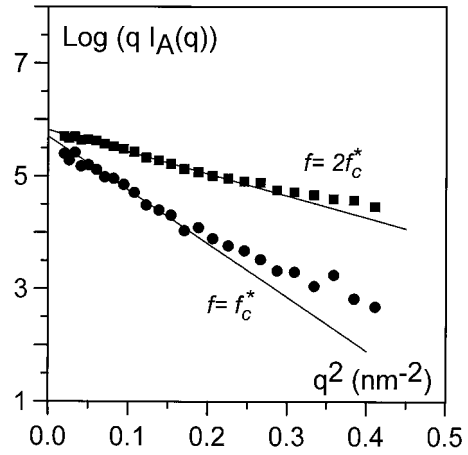


**Fig. 8.** Porod-plot (Log $qI_{\rm A}(q)$ *vs.* $q^2$) for the initial part of the scattering curves obtained for $f_{\rm c} = f_{\rm c}^*$(•) and for $f_{\rm c} = 2f_{\rm c}^*$(■).

The decrease in fibrils cross-section is therefore consistent, and actually expected, when heterogeneous nucleation is involved.

We first consider the case $f = 2f_{\rm c}^*$ for the sake of simplicity as it can be fitted with a simple model. The cross-section is found to be about $\sigma = 2.8 \pm 0.3$ nm while the mass per unit length is $\mu = 2200 \pm 200\,{\rm g\,mol^{-1}nm^{-1}}$, the latter value being about 4 times that of a chain under the *near*-$3_1$ helical conformation. At large angles, the behaviour can be fitted again by considering isolated chains whose scattering function is given by equation (3) for $qL > 1$ [18]. The fit yields $\mu_{\rm L} = 520\,{\rm g\,mol^{-1}nm^{-1}}$ and $r_{\rm H} = 0.45$ nm, values corresponding to the *near*-$3_1$ helical form. These results altogether suggest a model where four iPS chains encapsulate one bicopper complex monofilament as portrayed in Figure 8. The theoretical scattering curve can then be more explicitely written [23].

$$I(q) = \frac{\pi\mu_{\rm L}}{qn^2}\varphi(qr_{\rm H})\sum_j\sum_k J_0(qr_{jk}) \qquad (12)$$

where $n$ is the number of rod-like entities and $\varphi(qr)$ their cross-section scattering. Relation (12) becomes in the case of four chains distributed as shown in Figure 8:

$$q^2I(q) = \pi\mu_{\rm L}C_{\rm p}q\frac{4J_1^2(qr_{\rm H})}{q^2r_{\rm H}^2}[1+J_0(1.4qr)+2J_0(qr)]. \quad (13)$$

However, to produce a satisfactory fit of the entire scattering curve, one has to introduce some imperfections in the model, in particular to succeed in smoothing the strong oscillations of the theoretical curve, and also to retrieve the single chain behaviour at large-$q$. A possible approach is to consider frozen fluctuations of the distance between chains about the most probable value $l_0$. That such fluctuations are liable to account for the scattering curve can be shown by contemplating the following distribution function:

$$w(r) = l\exp(-l^2/2l_0^2) \qquad (14)$$

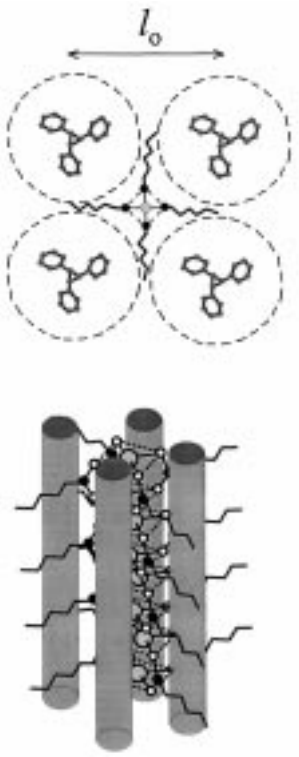


**Fig. 9.** Molecular model for the encapsulation of the bicopper complex by polymer chains: (upper) cross-section of the composite material: the bicopper complex and the iPS chains are seen parallel to the fibril axis. The dotted circles stand for the polymer solvation sheath. (lower) the model is seen perpendicular to the fibril axis. The chains are represented by means of greyish cylinders.

which is convenient for deriving an analytical solution for the scattered intensity by integration from 0 to $\infty$:

$$q^2I(q) = \pi\mu_{\rm L}C_{\rm p}q\frac{4J_1^2(qr_{\rm H})}{q^2r_{\rm H}^2} \times [1+\exp(-q^2l_0^2)+2\exp(-q^2l_0^2/2)]. \qquad (15)$$

Relation (15) gives the best fit shown in Figure 5 with $l_0 = 2.4$ nm by taking $r_{\rm H} = 0.45$ nm. The value of $l_0$ determined here is in very good agreement with the reported distance between first- neighbouring chains in the gel state. This rather large distance is the consequence of the existence of a *solvation shell* of *trans*-decalin molecules [6,21].

The schematic molecular model of a nucleated fibrils portrayed in Figure 9 can therefore account for the experimental scattering curves provided some allowance is made for the distance between the chains wrapping one given filament. The occurrence of frozen fluctuations is quite plausible as the chains most probably still possess the same conformation, that is a persistence length shorter than that of the bicopper filaments. This discrepancy is likely to introduce all sorts of distortions.

It is necessary to emphasize that this model is an average structure. Other forms of distribution than that of relation (14) may work as well, but also some degree of cross-section polydispersity is likely to come into play, although to a lesser extent than in the case of the non-nucleated fibrils. This is of no real concern in the present paper as these effects will not modify the essence of the above conclusions.

For $f_c = f_c^*$, the initial slope of the scattering curve in Figure 6 suggests that about 8 chains wrap one bicopper complex filament. The fit by means of equation (12) will not be attempted here due to the large number of intermolecular terms which renders the fitting procedure tedious, and to some extent useless since no new information are likely to be obtained.

Finally, the same types of scattering curves are observed for polymer concentration of $C_p = 0.08$ g/cm$^3$ and $C_p = 0.16$ g/cm$^3$ when prepared with bicopper complex concentrations corresponding to $f_c = f_c^*$ and $f_c = 2f_c^*$.

## Concluding remarks

We have reported on the method of preparation of a new type of composite material obtained *via* the heterogeneous nucleation by a self-assembling bicopper complex of the fibrillar structure of a thermoreversible gel prepared from solutions of a stereoregular polymer. Under these conditions, the copper atoms possess a one-dimensional, stabilized structure so that this composite material may possess the magnetic properties expected from spin ladders. Spin ladders, first described theoretically, are of prime importance as they may cast some light on the issue of high-$T_c$ superconductivity [21,22]. Measurements of magnetic susceptibility are in progress to assess this property in the composite material presented herein.

D. López is greatly indebted to the European Union for a post-doctoral grant in aid (TMR Programme). The authors are grateful to Dr. A. Brûlet from LLB (CEN Saclay) for experimental support while performing the neutron scattering experiments, and to Odile Gavat for the synthesis of the bicopper complex.

## References

1. C. Manfredi, M.A. Del Nobile, G. Mensitieri, G. Guerra, M. Rapacciulo, J. Polym. Sci. Polym. Phys. Ed. **35**, 133 (1997).
2. see for instance M.S. Dresselhaus, G. Dresselhaus, P.C. Eklund, *Science of Fullerenes and Carbon Nanotubes* (Academic Press, London, 1996).
3. J.M. Guenet, *Thermoreversible Gelation of Polymers and Biopolymers* (Academic Press, London, 1992).
4. E.D.T. Atkins, M.J. Hill, D.A. Jarvis, A. Keller, E. Sarhene, J.S. Shapiro, Colloid Polym. Sci. **262**, 22 (1984); J.M. Guenet, B. Lotz, J.C. Wittmann, Macromolecules, **18**, 420 (1985).
5. J.M. Guenet, Macromolecules **20**, 2874 (1987).
6. J.M. Guenet, Macromolecules **19**, 1960 (1986).
7. T. Nakaoki, M. Kobayashi, J. Mol. Struct **242**, 315 (1991).
8. H. Itagaki, I. Takahashi, Macromolecules **28**, 5477 (1995).
9. P. Terech, P. Maldivi, J.M. Guenet, Europhys. Lett. **17**, 515 (1992).
10. M.E. Cates, Macromolecules **20**, 2289 (1987).
11. P. Smith, P.J. Lemstra, J. Mater. Sci. **15**, 505 (1980).
12. G. Natta, J. Polym. Sci. **16**, 143 (1955).
13. R.L. Martin, H. Waterman, J. Chem. Soc. 2545 (1957).
14. J.P. Cotton, in *Neutron, X-ray and light scattering*, edited by Lindner, Zemb (Elsevier, 1991).
15. B. Fillon, J.C. Wittmann, B. Lotz, A. Thierry, J. Polym. Sci. Polym. Phys. Ed. **31**, 1383 (1993).
16. B. Fillon, B. Lotz, A. Thierry, J.C. Wittmann, J. Polym. Sci. Polym. Phys. Ed. **31**, 1395 (1993).
17. A. Thierry, C. Straupé, B. Lotz, J.C. Wittmann, Polym. Comm. **31**, 299 (1990).
18. C. Dammer, P. Terech, P. Maldivi, J.M. Guenet, Langmuir **11**, 1500 (1995).
19. G. Fournet, Bull. Soc. Franç. Minér. Crist. **74**, 39 (1951); O.A. Pringle, P.W. Schmidt, J. Appl. Crystallogr. **4**, 290 (1971).
20. H. Abied *et al.*, Liq. Cryst. **2**, 269 (1987).
21. J.M. Guenet, A. Menelle, V. Schaffhauser, P. Terech, A. Thierry, Colloid and Polym. Sci. **272**, 36 (1994).
22. J.M. Guenet, J. Phys. II France **4**, 1077 (1994).
23. G. Oster, D.P. Riley, Acta Crystallogr. **5**, 272 (1952).
24. J. Sagi, I. Affleck, Phys. Rev. B **53**, 9188 (1996).
25. G. Chaboussant *et al.*, Phys. Rev. Lett. **79**, 925 (1997).